HYDROLOGICAL PROCESSES
Hydrol. Process. **18**, 1447–1465 (2004)
Published online in Wiley InterScience (www.interscience.wiley.com). DOI: 10.1002/hyp.1422

Measurement, scaling, and topographic analyses of spatial crop yield and soil water content

Timothy R. Green* and Robert H. Erskine
US Department of Agriculture, Agricultural Research Service (ARS), Great Plains Systems Research Unit, 2150-D Centre Ave, Fort Collins, CO 80526 USA

Abstract:

The need to transfer information across a range of space–time scales (i.e. scaling) is coupled with the need to predict variables and processes of interest across landscapes (i.e. distributed simulation). Agricultural landscapes offer a unique set of problems and space–time data availability with the onset of satellite-based positioning and crop yield monitoring. The present study addresses quantification of the spatial variability of rainfed crop yield and near-surface soil water at farm field scales using two general methods: (1) geostatistical and fractal analyses; and (2) univariate linear regression using topographic attributes as explanatory variables. These methods are applied to 2 years of crop yield data from three fields in eastern Colorado, USA, and to soil-water content (depth-averaged over the top 30 cm) in one of these fields. Method 1 is useful for scaling each variable, and variogram shapes and their associated fractal dimensions of crop yield are related to those of topographic attributes. A new measure of fractal anisotropy is introduced and estimated from field data. Method 2 takes advantage of empirical and process knowledge of topographic controls on water movement and microenvironments. Topographic attributes, estimated from a digital elevation model at some scale (10 m by 10 m spacing here), help explain the spatial variability in crop yield. The topographic wetness index, for example, explained from 38 to 48% of the spatial variance in 1997 wheat yield. Soil water displays more random spatial variability, and its dynamic nature makes it difficult to predict in both space and time. Despite such variability, spatial structure is evident and can be approximated by simple fractals out to lag distances of about 450 m. In summary, these data and spatial analyses provide a basis and motivation for estimating the fractal behaviour, spatial statistics, and distributed patterns of crop yield from landscape topographic information. Published in 2004 by John Wiley & Sons, Ltd.

KEY WORDS landscape topography; crop yield; soil moisture; spatial data; scaling; fractals; hydrology; agriculture

INTRODUCTION

Problems associated with space–time variability and scaling across watersheds and landscape areas are ubiquitous. Understanding of scaling behaviour and space–time interactions is critical for addressing differential site-specific management of areas within fields (i.e. 'precision agriculture' with variable-rate inputs) and regionalization across fields. Quantifying observed space–time interactions is important for sustainable land management in terms of both agronomic production and environmental protection. Agricultural landscapes and practices offer some unique opportunities to collect, analyse and simulate spatial data within and among fields, particularly with the availability of satellite-based positioning and spatial crop yield monitoring.

Variability in crop yield stems from nonlinear spatial interactions between numerous factors, including topographic relief, precipitation, soil hydraulic properties, nutrients and organic matter. Such factors cause variability at nested scales that may give rise to a self-similar pattern of variation described by fractal geometry (Mandelbrot, 1977; Burrough, 1983). Such fractal behaviour can be quantified using simple parameters (e.g. fractal dimension), which are useful for characterizing data such as crop yield and for quantifying scaling

* Correspondence to: Timothy R. Green, US Department of Agriculture, Agricultural Research Service (ARS), Great Plains Systems Research Unit, 2150-D Centre Ave, Fort Collins, CO 80526, USA. E-mail: green@gpsr.colostate.edu

Received 10 May 2002
Accepted 15 January 2003

relationships with landscape variables. Plant-available soil water is also the primary limiting factor for crop growth and yield in semi-arid landscapes, so we address the space–time behaviour of near-surface (top 30 cm) soil water in this context.

In this study, we will show that landscape topography reveals spatial patterns visually similar to crop yield. We then use variogram and fractal analyses to explore the spatial characteristics of topographic attributes estimated from elevation data in a 10 m digital elevation model (DEM). The overall spatial statistics and fractal dimensions, including their anisotropy, are compared to show relationships between more readily available topographic data and crop yield or soil water. This is followed by direct correlations between spatial variables to predict spatial patterns of crop yield from topographic attributes and to explain part of the total variance. The portion of spatial variance explained can be important for future applications of classifying land areas for differential management.

Previous hydrological studies

Spatial scaling of variables such as surface soil moisture has been an important topic in the hydrological literature (e.g. Blöschl and Sivapalan, 1995; Sposito, 1995; Blöschl *et al*., 1997). The growing field of ecohydrology also highlights interest in understanding and quantifying soil–water–plant process interactions, including the role of landscape variability in patterns of ecohydrological variables. Yet, high-resolution spatial measurement of plant variables in the field, other than crop yield, is uncommon.

In the context of runoff generation, Woods and Sivapalan (1997) investigated spatial distributions of the topographic wetness index (defined and used below), found a power-law form of its cumulative distribution for each catchment, and related the exponents to the degree of spatial organization within a catchment. Soil moisture organization within a pasture (10·5 ha) has also been related to topographic attributes (Western and Grayson, 1998; Western *et al*., 1999). Western *et al*. (1999) identified the strongest univariate correlation with log-transformed contributing area under wet conditions in a shallow soil with lateral saturated flow convergence. Blöschl (1999) addressed the inference of patterns from variogram analyses within a broader context of scaling issues in snow hydrology. Likewise for soil moisture, Western and Blöschl (1999) addressed biases in estimated correlation length and variance due to the measurement scale (support, spacing and extent). Furthermore, they affirmed the applicability of geostatistical techniques for predicting such bias in the presence of spatial organization, including connectivity.

Others have scaled soil moisture independently using field measurements and remotely sensed data (Rodriguez-Iturbe *et al*., 1995; Hu *et al*., 1997, 1998; Pelletier *et al*., 1997; Cosh and Brutsaert, 1999; Oldak *et al*., 2002), and simulations of such data (Wood, 1995; Peters-Lidard *et al*., 2001). Cosh and Brutsaert (1999) analysed the Washita '92 experimental data using variograms. They concluded that soil moisture in the region (18×25 km^2) was nonstationary with fractal behaviour, but could be considered stationary for distances below 5 km. That is, some of the nested scales were relatively discrete rather than continuous. Recently, Bindlish and Barros (2002) applied fractal scaling to L-band ESTAR data and were able to downscale from 200 m to 40 m, which is similar to the scales of the present study. Peters-Liddard *et al*. (2001) also used remotely sensed data and modelled soil moisture to demonstrate (multi)fractal behaviour in space with distinct dry-down regimes in time, indicating a transition from simple scaling to multiscaling. At a larger scale, Rodriguez-Iturbe *et al*. (1998) and D'Odorico and Rodriguez-Iturbe (2000) also found self-organization and space–time scaling in simulated hydrologic states (including soil moisture) that agreed with available field observations. Overall, simple scaling and multiscaling are common features of these studies; the approach remains empirical; and the results are site specific. Further investigation of the scaling behaviours and interrelationships between water, plant, and topographic variables is needed to help quantify and address observed space–time variability.

Site description

The three fields used in this study are part of the Lindstrom farm located in eastern Colorado, USA (40·37 °N, 103·13 °W). The climate is semi-arid with an average pan evaporation of approximately 1600 mm per growing

season, whereas the average annual precipitation (1961–90) is only 440 mm (Peterson *et al.*, 2000). The terrain is generally undulating with aeolian deposits of silt- and sand-sized material mantling sedimentary rock (primarily sandstone) and fluvial deposits of the South Platte River basin. The unconsolidated sediment and soils in our study fields are relatively thick (at least 3 m) with little or no surface expressions of groundwater or perched water in the root zone. Thin calcareous horizons have been sampled at depths of 20–50 cm, but soil horizons are not very pronounced otherwise. The relief is greatest in the 'North' field (21·3 m over 63 ha), where the elevation ranges from approximately 1361 to 1382 m, with slopes exceeding 14%. The 'South' field (72 ha) and 'West' field (36 ha) have total relief values of 10·9 m and 8·5 m, respectively.

METHODS

Although the findings here are directly applicable only to dryland cropping at this location, the same concepts and methods should apply to other semi-arid climates. It is worth noting that the soils and climate are not ideal for application of static indices, such as the steady-state 'wetness index' used below. However, such topographic attributes may be useful for quantifying a portion of the observed variability in soil water and crop yield. The methods below are divided into measurements of different individual landscape variables, then into methods of spatial statistical/fractal analyses and univariate regression.

Measurements

Crop yield monitoring on the Lindstrom Farm began in 1997, and more concerted efforts to measure the soils, soil-water content and topography began in 1999. The work presented here focuses on spatial measurement of elevation, near-surface (30 cm deep) water content, and crop yield.

Elevation. Elevation data were collected using dual-frequency, real-time kinematic global positioning system (GPS) receiver mounted on an all-terrain vehicle. Raw elevation data of approximately 5 m resolution (horizontal measurement spacing) for the North field and 10 m resolution on the South and West fields were interpolated using kriging onto a 10 m × 10 m grid DEM. The experimental variogram out to a separation distance of 30 m was fit to a Gaussian model. Cross-validation of this interpolation method resulted in root-mean-squared errors of 0·036 m, 0·054 m, and 0·038 m on the North, South, and West fields respectively.

Crop yield. We collected spatial yield data for winter wheat on all three fields in 1997, and wheat on two fields and foxtail millet on one field in 1999. Winter wheat was harvested using a 9 m wide combine header and measured with a yield monitor (MicroTrak Systems Inc.) linked to a GPS receiver with satellite (OmniStar™) differential correction. Each data point is an instantaneous value of grain flow across the auger-mounted sensor, which is converted and calibrated to a mass per unit area (Mg ha^{-1} or bushels/acre). The data 'points' have a small, unknown support scale associated with averaging grain flow from across the header and in the direction of travel. Several investigators have identified a time lag and tested the accuracy of spatial grain yield measurements (e.g. Arslan and Colvin, 1999; Beal and Tian, 2001), and modern yield monitors have a default time-lag correction (e.g. 12 s). The sampling interval is typically 3 s, so measurement spacing in the direction of travel varies with the combine ground speed. Values from irregular yield data were interpolated using kriging onto the uniform 10 m DEM grid.

Foxtail millet (hay) was baled in the North field in 1999. A sample of the hay bales was measured for volume, water content and weight to determine the dry weight per bale. Bale locations were located with a satellite-differential GPS receiver to determine the harvest area. Details of the yield mapping methods have been reported previously (Erskine *et al.*, 2001). These geo-referenced bale data have large support scales, unlike grain yield data.

Surface soil moisture. Spatial soil moisture was measured only on the North field. Soil water contents were measured using time domain reflectometry (TDR) with 30 cm rods in the spatial pattern shown in

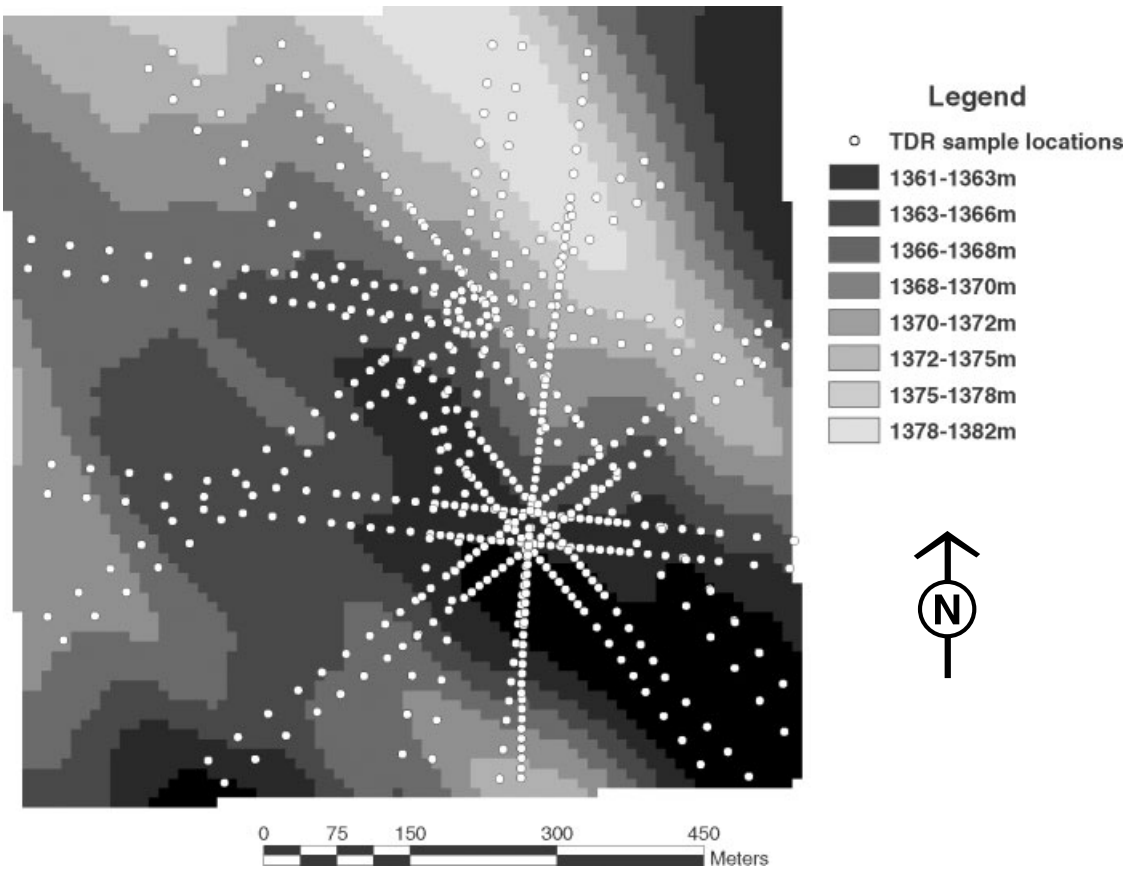

Figure 1. TDR measurement locations (symbols) on a map of North field elevation

Figure 1 for each sampling period (one or two days each). The TDR probes were inserted using a hydraulic coring device (Giddings Machine Co.) mounted on a six-wheel ATV (John Deere Gator™) similar to that of Western and Grayson (1998). A satellite differential GPS receiver (Pathfinder Pro XRS™ by Trimble) was used for navigation to sample points, and data logging was integrated with the TraseBE™ TDR instrument (Soil Moisture, Inc.), making rapid measurement possible. Values of water content were computed from a universal calibration curve for all data reported here.

Data analyses

Our focus in this paper is on analyses of the spatial attributes and relationships between landscape topography, crop yield and soil moisture. Limited space–time analyses are possible using two harvest years over three fields. However, we explore regional (spatial) and temporal similarity between crop years, as well as space–time variability within a field for soil moisture at discrete sample dates. First-order topographic relationships with crop yield and soil moisture are also highlighted.

Computing topographic attributes. Topographic attributes can be computed using a DEM and geographical information system (GIS) software. Estimates of local slope S and specific contributing area α, defined as the upslope contributing area per unit contour length, were computed using TARDEM (Tarboton, 2000) implementing the D_∞ method for flow direction (Tarboton, 1997), with and without sink filling. The specific

contributing area values were log-transformed, as per Western *et al*. (1999), to remove the extreme skewness in the frequency distribution. The topographic wetness index WI is defined as

$$\mathrm{WI} = \ln\left(\frac{\alpha_{\mathrm{f}}}{S}\right) \tag{1}$$

where the subscript on α_{f} denotes sink filling. The aspect and plan and profile curvatures were computed using TAPES-G (Gallant and Wilson, 1996). The total curvature was computed using a central finite difference (Gerald, 1980: 206).

Experimental variograms. Analyses of experimental variograms and model fits were performed using power-law variograms without any nugget (i.e. the variance at zero lag equals zero) for all data types (elevation, crop yield, and soil water content) to facilitate consistent fractal analyses. In most cases, the experimental variograms could be fit relatively well with a two-parameter, power-law variogram model:

$$\gamma(h) = ah^b \tag{2}$$

In the case of elevation, however, Gaussian variograms fit the data better. To test for anisotropy, the procedure was repeated with directional variograms for angles of 10, 55, 100 and 145° east of north (see TDR sample patterns in Figure 1).

Fractal analysis. There are numerous methods to test whether spatial variability follows a fractal behaviour (e.g. Barton and LaPointe, 1995). In this study, we used the approach of Burrough (1981, 1983). Briefly, the characteristics of fractional Brownian motion are that sequential increments $(Y(x+h) - Y(x))$ must have a Gaussian distribution with zero mean and variance σ^2, and have a variogram that can be adequately described by

$$2\gamma(h) = E[Y(x+h) - Y(x)]^2 = \sigma^2 h^{2H} \tag{3}$$

where $Y(x+h)$ and $Y(x)$ are values of yield (or other variables) at locations $x+h$ and x, E is the expectation operator, and H is a scaling parameter known as the Hurst exponent (Karner, 2001; Koutsoyiannis, 2002). It follows that a power-law fit of the semivariogram versus lag h indicates fractional Brownian motion. For measurements along a transect, the fractal dimension is

$$D = 2 - H \tag{4}$$

where $2H$ is the exponent b of the power-law model (Equation (2)).

By this definition, and to be consistent with Burrough (1981, 1983), the fractal dimension can range from 1 to 2, because variability is measured between points at given spatial lags along each radial direction. When $D = 1{\cdot}5$, for example, H is 0·5 and the variogram is linear ($\gamma = ah$). Values of $H > 0{\cdot}5$ (i.e. $D < 1{\cdot}5$) represent increased spatial 'persistence' or smooth features with dominantly large-scale variations filling less of the two-dimensional space. Conversely, values of $H < 0{\cdot}5$ (i.e. $D > 1{\cdot}5$) represent anti-persistence. Values of D approaching 2·00, here, indicate spatial randomness or 'noise' filling a two-dimensional space. Interpreted another way, the reader may view the measured variability as occurring on a surface, instead of along a line, and add 1 to the D values computed here. However, fractal dimensions from directional variograms do not span a three-dimensional space.

Given the above equivalence between a log–log linear variogram and a fractal dimension, we note that there must be an equivalent anisotropy in the spatial correlation or persistence. To quantify this anisotropy, we propose the following:

$$\text{Fractal anisotropy} \quad \triangleq \quad \sqrt{10^{b_{\min}}}/\sqrt{10^{b_{\max}}} = \sqrt{10^{(b_{\min}-b_{\max})}} = \sqrt{10^{2\Delta D}} = 10^{\Delta D} \tag{5}$$

where $\Delta D = D_{\max} - D_{\min}$, and $b_{\min}$ and $b_{\max}$ are the minimum and maximum values respectively of the exponent b (Equation (2)) in the principal directions. Noting that the fractal dimension is independent of the variogram units or scale (i.e. a), we assume a fixed value of a, such that

$$\left.\sqrt{\frac{\gamma_{\max}(h)}{\gamma_{\min}(h)}}\right|_a = h^{\Delta D} = 10^{\Delta D \log h} \tag{6}$$

where the left-hand side is the square-root of the ratio of semi-variances in the principal directions for a given value of a. Thus, our measure of fractal anisotropy (Equation (5)) has some physical significance as a ratio of the standard deviation between measurements in orthogonal directions at a given lag distance (i.e. $h = 10$). It is also a practical quantity equal to 1·0 for isotropic conditions and increasing with the degree of anisotropy to a theoretical maximum of 10. As shown below, the fractal anisotropy does not exceed 4·0 in the cases studied here, and is commonly less than 2.

Univariate regression. Wheat yield for 1997 was regressed on topographic attributes computed from DEMs of all three fields with 20% of the extreme values trimmed to help remove bias in the correlation and provide a robust estimate (Rousseeuw, 1984; Mayo and Gray, 1997; Insightful, 2001: 155; Giloni and Padberg, 2002). Additional data trimming (up to 40%) caused reduced values of r, which are not reported. Univariate linear correlations were also computed for soil moisture on the North field for 1999–2000.

We then explored the following exponential model as an alternative to the linear model for yield:

$$Y \sim \mathrm{e}^{-5X^*} \tag{7}$$

where Y is crop yield and $X^* = (X - X_{\min})/(X_{\max} - X_{\min})$, where X is one of the six topographic attributes. The multiplier of 5 provides a range of [0·0067, 1·0] for the transformed explanatory variable.

The regression analyses presented here ignore the effects of spatial covariance between dependent and explanatory variables. We also do not address or take advantage of spatial averaging of measurements over areas above the measurement scale. For example, one may wish to predict crop yield averaged over 1 ha areas from an average of one topographic attribute (or more, in the case of multivariate regression) over the same areas. These issues are left for topics of future investigation.

RESULTS AND DISCUSSION

The results are organized and discussed in the following manner. First, we present some of the basic spatial data, including grain yield in 1997 and soil-water TDR measurements in 1999. Experimental variograms and model fits are then presented for each spatial variable independently. Changes in the spatial auto-correlation with time are noted where applicable. The power-law variograms are then used to estimate fractal dimensions and anisotropy values for each variable. Fractal properties are compared between yield in 1997 and 1999, soil water at different dates, and six topographic attributes. We explore estimating fractal dimensions and variogram parameters of yield from given topographic attributes. Finally, point-to-point spatial regressions are performed between yield and each topographic attribute, and between soil water by date and each topographic attribute.

Space–time data

Figure 2 is presented as motivation for exploring spatial relationships between crop grain yield, which may be a surrogate for temporally averaged soil water in the root zone, and static attributes of the landscape topography. The top row of Figure 2 shows 1997 winter wheat yield overlaid on the field topography (elevation), followed by the bottom row of the topographic wetness index WI overlaid on the same topography

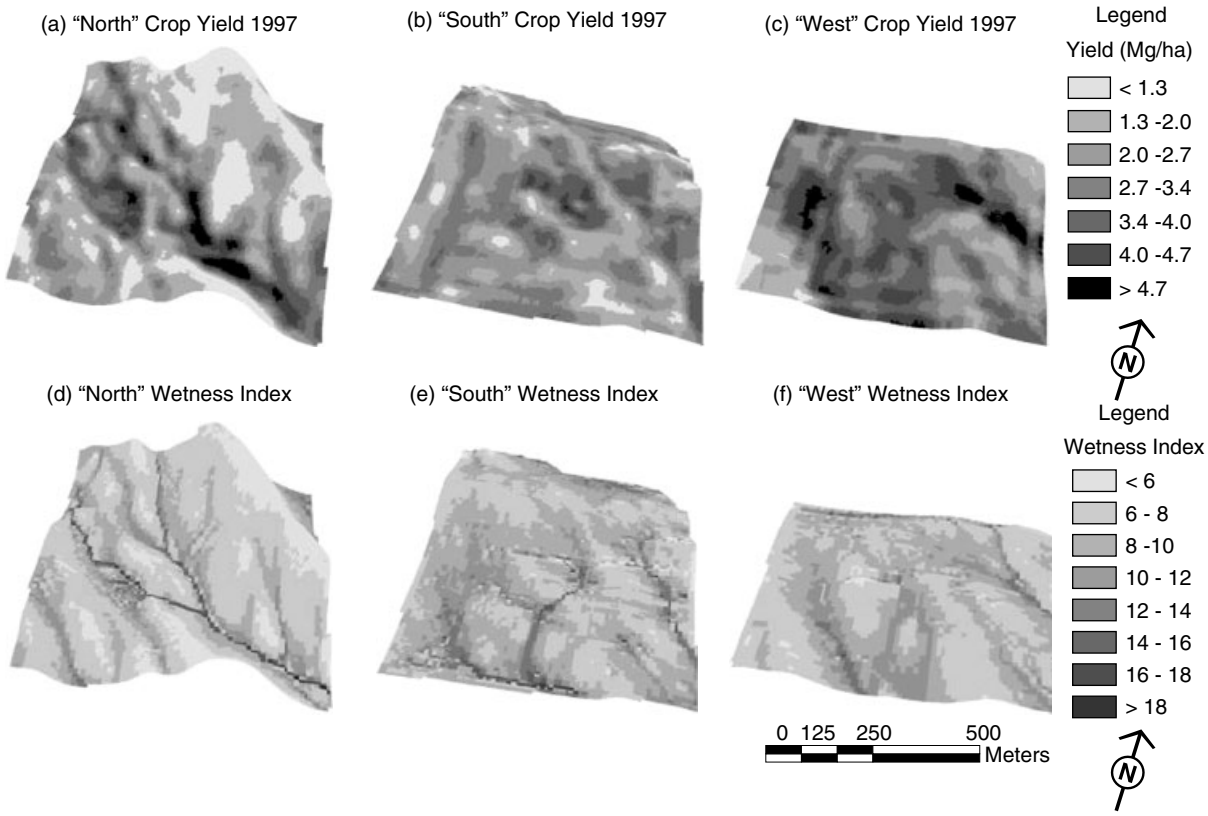

Figure 2. Winter wheat grain yield for 1997 (a–c) and topographic wetness index (d–f) overlaid on the topography of three fields: North (a, d), South (b, e), and West (c, f). Topographic relief is exaggerated 10 times for all images

for each of the three fields. On the North field (Figure 2a and d), one can readily (visually) follow drainage lines on the WI map up small subcatchments and see corresponding patterns on the yield map. Upon careful inspection, such features are seen across all three fields, including the West field (Figure 2c and f) with the least topographic relief. These empirical relationships occur despite violating the theoretical steady flow assumption used to derive WI. Although WI is computed from present-day elevation alone, it may reflect both long-term soil deposition patterns and shorter-term water accumulation associated with infrequent runoff events and lateral unsaturated flow (despite having deep soils with no obvious impeding layers). The crop at each location also reflects some temporal average of high-frequency variations in soil water.

The soil-water data collected in 1999 are summarized by the histograms in Figure 3. During the early growth stages in late June (Figure 3a), the crop had not yet used much stored water, and the distribution was skewed to the left. Just 2 weeks later, in mid-July (Figure 3b), the distribution was more symmetrical, but late-July rainfall increased soil water in early August (Figure 3c). Finally, after harvest and very little rain (Figure 3d), the soils were dry, and the distribution skewed to the right.

Winter wheat is planted in furrows divided by small 'ridges' without plants. Furrow-to-furrow spacing is approximately 30 cm. Figure 4 shows that the sample micro-location does not cause a large bias. The furrows tend to be slightly wetter than ridges (Figure 4a and d), but this small bias was reversed on one sampling date (Figure 4b) and practically non-existent on the next (Figure 4c). Thus, we neglect this relatively minor source of small-scale variability in the analyses below.

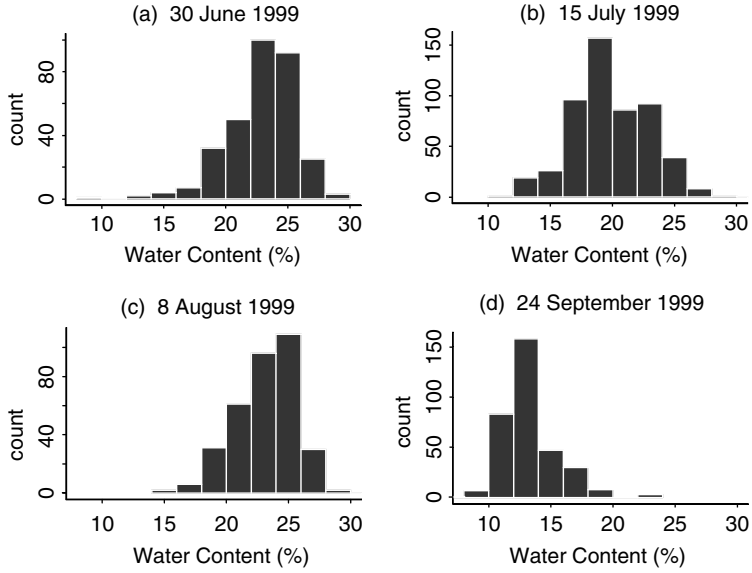

Figure 3. Frequency histograms of measured water content (30 cm TDR) for four sample dates and moisture states

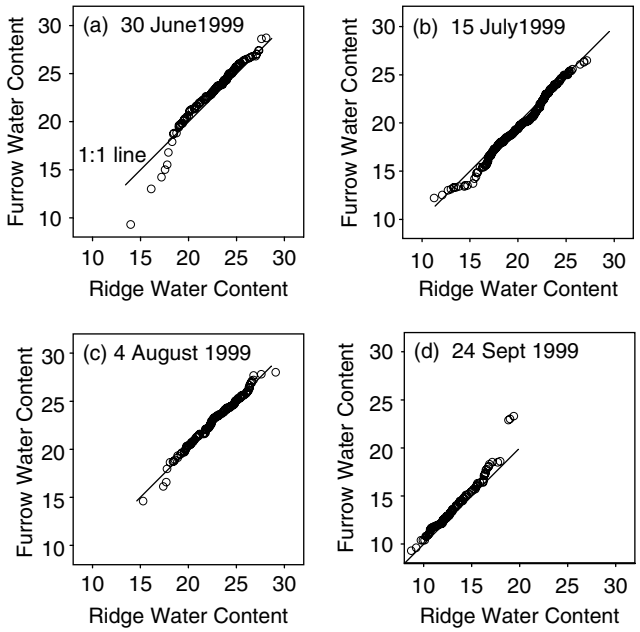

Figure 4. Furrow effects on TDR-measured water contents (top 30 cm) showing furrow versus ridge water contents (symbols) around 1 : 1 lines for four sample dates in 1999. Units of water content are percent volumetric ($100 \times m^3\ m^{-3}$)

Experimental variogram analysis

The spatial statistical structures of elevation, crop yield and TDR data are analysed using experimental variograms and model fits. In Figure 5, the experimental variograms (Figure 5b–e) include data pairs in a 45° view. The Gaussian variogram model fits the experimental variograms of elevation best over the full

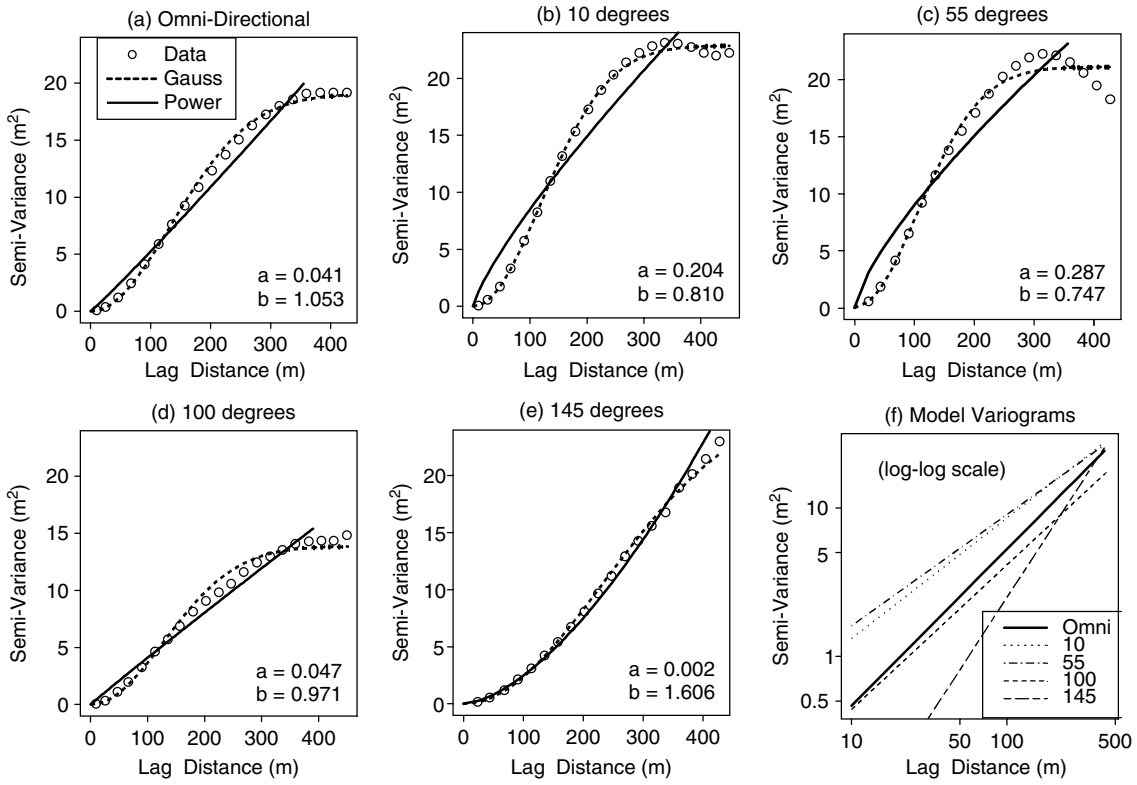

Figure 5. North field elevation experimental variograms and model fits using power-law (for fractal analysis below) and Gaussian models for omnidirectional (a) and directional cases (b)–(e). Parameter values of the power-law fits are shown as *a* and *b*

range due to an apparent sill (Figure 5a and d) or periodic behaviour (Figure 5b and c). Power-law model fits are compared with each other on a log–log plot (Figure 5f), where 'Omni' is the omnidirectional case for all data compared with 10, 55, 100 and 145° east of true north. There is significant anisotropy due to the prevailing summit and swale directions, typically toward the southeast. Some of this effect could be removed with universal kriging, but not using a simple linear trend. Furthermore, nonstationary behaviour is expected for this domain size, and it is reflected in the power-law variogram model. The multiplier *a* and exponent *b* of the power-law model are shown in each variogram plot.

Despite such sill and periodic behaviour for elevation on the North field in two or three directions, variograms of slope on the same field (Figure 6) display nested scales of variance with no apparent sill in all directions. These plots and model fits are typical of the results for the South and West fields as well.

Variograms for the North field winter wheat in 1997 are shown in Figure 7. The power-law model fits the omnidirectional data (a) well, with its monotonic structure and small nugget. The directional variograms (Figure 7b–e) display anisotropy in the spatial correlation structure with principal directions likely falling in the ranges 10–55° and 100–145°. The omnidirectional fit (neglecting anisotropy) falls nicely between these two extremes, as seen in Figure 7e. Foxtail millet data for 1999 also display spatial structure that is fit well by the power-law model in Figure 8. The omnidirectional fit to all data is very good, and gives parameters very similar to those for the 100° direction. In fact, the bearing of the baler path was approximately 145°, which may contribute to the observed anisotropy.

Variograms of TDR data also displayed anisotropy, but Figure 9 shows only the omnidirectional variograms for each sample date in 1999. The power-law model fits all but the June 24 sample (Figure 9a) relatively well,

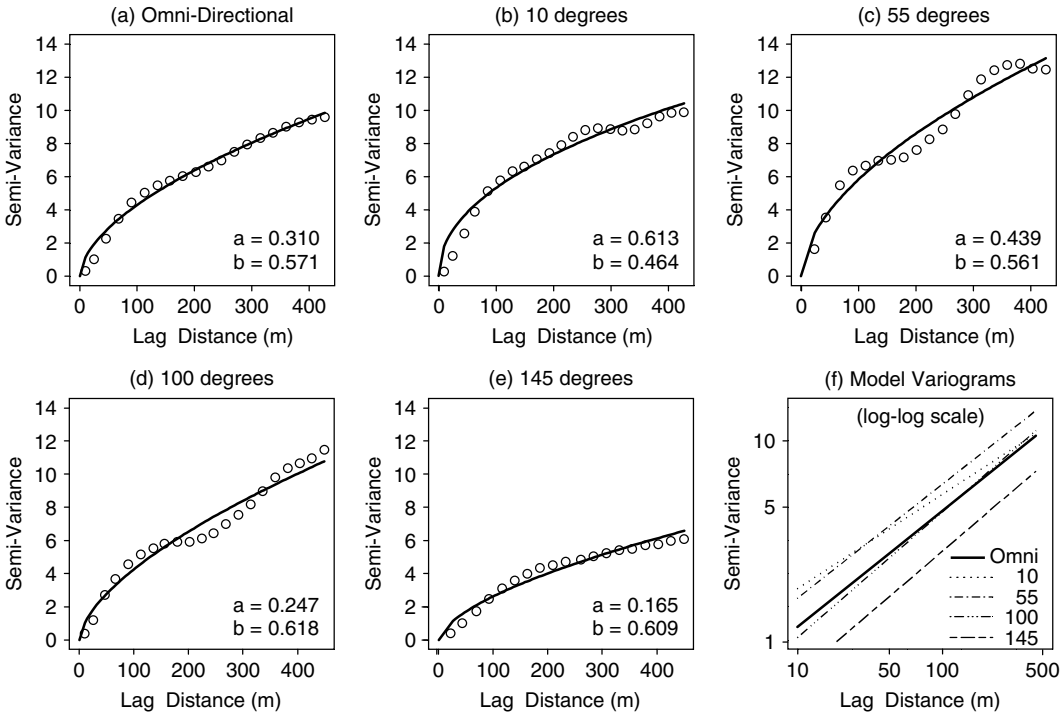

Figure 6. North field slope experimental variograms and power-law model fits for omnidirectional (a) and directional cases (b)–(e). Parameter values of the power-law fits are shown as a and b. Units of semi-variance are $(\mathrm{m\ m^{-1}})^2$ or dimensionless

with the longest correlation lengths and best fits when it was relatively wet (Figure 9b and d). Figure 9f shows variability in both the slope and magnitude of the log-variograms. Yet, it is interesting to note the similarity in slopes ($b = 0{\cdot}135$ and $0{\cdot}137$) between a relatively wet date (4 August) and a dry date (24 September). Finally, there is marked spatial auto-correlation over a broad range of length scales in the experimental variograms for all dates, with the possible exception of 15 July (Figure 9c), where the moisture regime was oscillating between wet and dry conditions due to plant water uptake and summer rains. Such conditions may tend to disrupt any spatial organization that develops over longer time scales. The power-law model may be questionable in this case, but it is used for comparison with other dates, and to compute a fractal measure of the spatial variability.

Fractal properties

Values of the fractal dimension D are given in Table I for crop yield (1997 and 1999) and topographic attributes over all three fields. Table I shows the power-law variogram model parameters a and b for the omni-directional ('Omni') fits only, but computed values of D in four directions are also given. The last column provides a measure of the statistical/fractal anisotropy of each attribute based on the range of D values (see Equation (5)). Although the direction of anisotropy is not always consistent, it tends to favour one direction for each field, and the minimum value of D for each attribute is noted using italics in Table I.

The omnidirectional fractal dimensions range from $1{\cdot}28$ for elevation in the North field to $2{\cdot}00$ for topographic curvature in the West field. The former reflects strong spatial persistence in the elevation of this undulating terrain, i.e. smooth topographic features and large-scale variations relative to the field size, whereas the latter reflects almost no spatial persistence in the rate of change of slopes. On the North field, $D = 1{\cdot}86$ for wheat yield in 1997, and $D = 1{\cdot}83$ for millet in 1999. The reduced value of D in 1999 is likely due to the relatively large support scale for each measured hay bale. Yield in both years displays much less

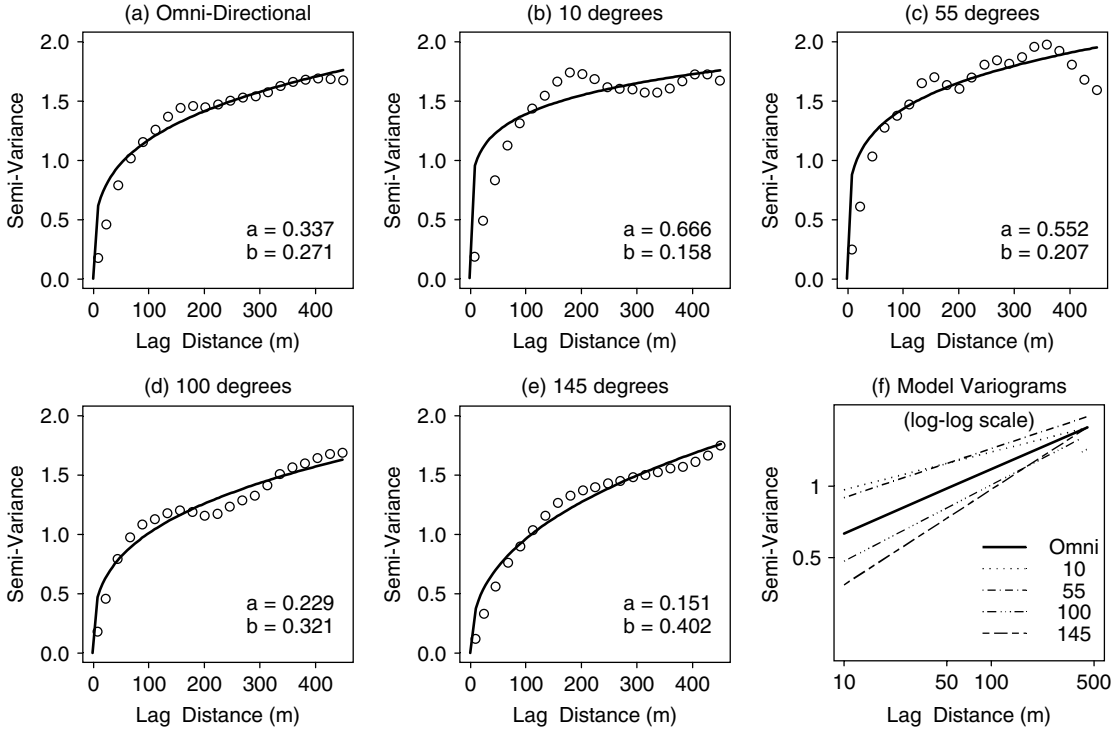

Figure 7. North field winter wheat grain yield data (1997) showing experimental variogram fits as per Figure 6. Units of semi-variance are $(\text{Mg ha}^{-1})^2$, and the b parameter value is not affected by units of yield

spatial persistence than elevation, more persistence than curvature, and fractals values between S and either $\ln(\alpha)$ or WI.

In conjunction with Table II, Figure 10 shows the variability of mean water content and D with time. Again, we note a rapid increase in anti-persistence during July, followed by more spatial persistence later in the season under both wetter and drier mean conditions. In the water-limiting growth conditions of our dryland agriculture, we would seek for some relationship between a temporal mean of D for water content and the value of D for crop yield in that year. However, crop yield ($D = 1{\cdot}86$) is more spatially persistent than water content on any given sample date. The nearest similarity between crop yield and soil water ($D = 1{\cdot}88$) occurs early in the season, during crop emergence. This is when the plant is most affected by near-surface moisture (e.g. top 30 cm measured by TDR)—versus later in the season, when plant roots find deeper water—and ultimate yield can be sensitive to emergence rates in dryland agriculture (McMaster *et al.*, 2002).

Another pattern is found in the anisotropy measure for crop yield and certain topographic attributes in Table I. The anisotropy in spatial persistence of crop yield is lowest for the South field in both years. This is consistent with the contributing area and WI statistics, but not with elevation and its first two spatial derivatives. The anisotropy measure is greatest, by far, for elevation in the West field, where D is the lowest ($1{\cdot}09$) at 145°, corresponding to the predominant direction of topographic features in this relatively flat field.

Finally, topographic curvature, which appears to display little spatial persistence ($D = 1{\cdot}95$, $1{\cdot}96$ and $2{\cdot}00$ for the South, North and West fields respectively), contains relatively strong continuity in very narrow features, particularly on the North field. Comparison of Figure 11 with Figure 2d reveals topographic inflections along ridges and drainage lines. Additional features in Figure 11 reflect smooth terraces perpendicular to the steepest slopes. The magnitude and direction of anisotropy (Table I) are consistent with these features in the curvature map.

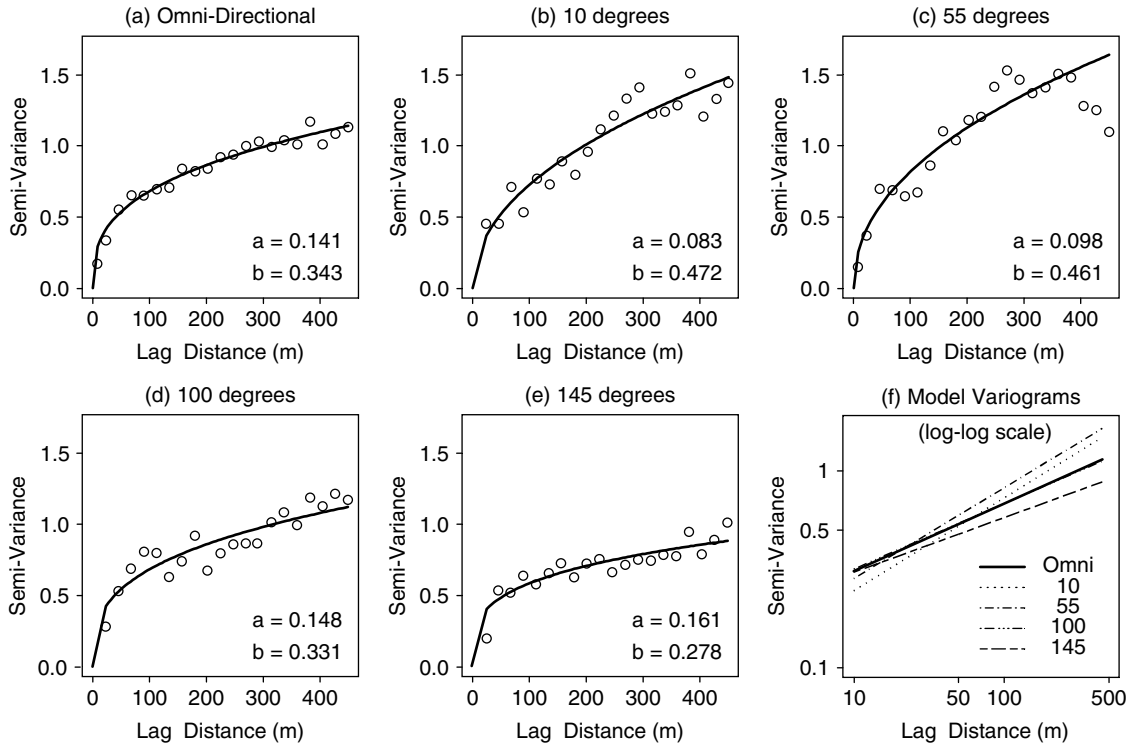

Figure 8. North field foxtail millet (hay) yield data (1999) showing experimental variogram fits as per Figure 6. Units of semi-variance are $(\text{Mg ha}^{-1})^2$

Relating fractal behaviour of yield to topography

Given the analyses above, it is possible to explore relationships between the lumped spatial statistics measured using the fractal dimension. Some trends and similarities between values of D for different variables were identified above. Here, we explore the potential for estimating fractals and generalized variograms of yield from those of topography.

Table III shows selected ratios of spatial statistical parameters for all three fields. The second column in Table III uses limited temporal data (2 years) to indicate a degree of temporal stability in yield spatial autocorrelation between 1997 and 1999. The fractal dimensions for yield did not vary much in time for the South and West fields, where the wheat–fallow rotation continued. The ratio was lower for the North field (0·98), where different crops were planted in the years following 1997, and due to the increased support scale of hay bale measurements.

The omnidirectional D values for WI were similar to those for 1997 yield in all three fields, with an average ratio of 1·016. Thus, WI may be a useful topographic attribute for estimating typical fractal behaviour of wheat grain yield in fields, at least within this region.

Scaling of variograms may also be possible, but the ratios of b values between WI and yield are more variable and not near unity. This is largely due to the mathematics of the ratios of differences. For example, if we have two D values of 1·998 and 1·999, their ratio is 0·9995, but the ratio of corresponding b values (from Equations (3) and (4)) is $0{\cdot}004/0{\cdot}002 = 2$. However, the shapes of the variograms are similar. The next question is: Can one estimate the magnitude or scale of semi-variance given the variogram shape associated with D? The ratios of a values in Table III are all near 3, which provides motivation to investigate further the concept of estimating the full variograms along with the fractal behaviour measured by D.

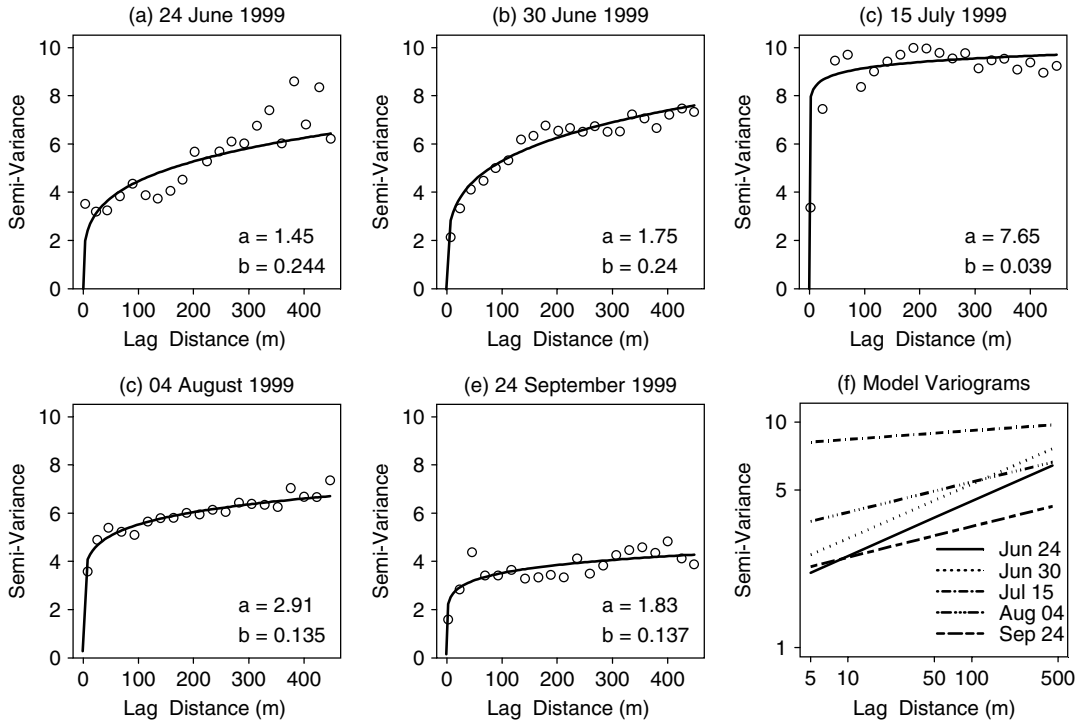

Figure 9. Soil water content for five sample dates (a)–(e), and a composite of all five dates on a log–log plot (f). Units of semi-variance are $(100\ m^3\ m^{-3})^2$

Mapping crop yield and soil water content from topographic attributes

Recalling the patterns in Figure 2, we expect spatial crop yield to be correlated with one or more topographic attributes. In this paper, we explore univariate point-to-point correlations by joining dense, but irregularly spaced, yield data to the nearest 10 m DEM grid points. Figure 12 shows the resulting scatter plots of pairs of North field 1997 wheat yield versus each topographic attribute. There is quite a bit of noise in each of these relationships, but there is also apparent correlation. The scatter plots also indicate some nonlinearity, for which exponential transformations (Equation (7)) are used.

Thus, yield is regressed on each topographic attribute independently, and linear analyses are performed for soil-water content. Table IV gives detailed results from regressions between the 1997 crop yield and topographic attributes. Results of linear regression (rows in bold) are compared with nonlinear regression (non-bold rows). Spatial means and standard deviations of the regressed variables are also reported. The coefficient of variation for wheat yield in the North field is 0·57, compared with 0·37 and 0·35 for the South and West fields respectively.

Greater variability in the North field may provide opportunity for improved, site-specific management (i.e. 'precision agriculture') by using topographic classification to delineate land management units with different input rates. In any case, topographic relief, slope and curvature provide more explanatory power (individually) in the North field than with the other two fields. However, the correlation with contributing area (with and without sink filling) is greater on the other fields. The direction of correlation (positive or negative) is consistent for each topographic attribute across all three fields. Yield is negatively correlated with Z and S, and is positively correlated with the other topographic attributes. The exponential transformation of variables (Equation (7)) causes the sign of the r-values to change compared with the r-values resulting from linear regression. Nonlinear regression was advantageous only for Z and S.

Table I. Values of variogram parameters and fractal dimensions for crop yields and topographic attributes computed from a 10 m DEM for each field (N = North, S = South, W = West): 'Omni' denotes omnidirectional variogram fits, and the numbers 10, 55, 100, and 145 are degrees east of true north (±180°). The lowest value of D from directional variograms is italicized for each attribute and field. The last column is a measure of fractal anisotropy. N* denotes a different crop (hay millet, instead of winter wheat) on the North field in 1999. Z is elevation, S is slope, C is total curvature, $\ln(\alpha_s)$ and $\ln(\alpha_f)$ are natural logarithms of specific contributing area with sinks and filled sinks respectively, and WI is the wetness index defined as $\ln(\alpha_f/S)$

Attribute	Field	Variogram (Omni)		Fractal dimension D					$10^{\Delta D}$
		a	b	Omni	10°	55°	100°	145°	
1997 yield	N	0·337	0·271	1·86	1·92	1·90	1·84	*1·80*	1·32
	S	0·253	0·196	1·90	1·93	1·92	1·91	*1·85*	1·20
	W	0·424	0·185	1·91	2·00	1·87	*1·82*	1·99	1·51
1999 yield	N*	0·142	0·341	1·83	*1·76*	1·77	1·83	1·86	1·26
	S	0·202	0·195	1·90	1·92	1·88	*1·88*	1·93	1·12
	W	0·271	0·205	1·90	1·88	1·96	1·92	*1·83*	1·35
Z	N	0·411	1·053	1·47	1·60	1·63	1·51	*1·50*	1·26
	S	$8{\cdot}40 \times 10^{-5}$	1·447	1·28	1·42	1·37	*1·18*	*1·18*	1·74
	W	$2{\cdot}22 \times 10^{-4}$	1·264	1·37	1·35	1·69	1·43	*1·09*	3·98
S	N	0·310	0·571	1·71	1·77	1·72	*1·69*	1·70	1·20
	S	0·171	0·288	1·86	1·85	2·00	*1·77*	1·80	1·70
	W	0·147	0·304	1·85	1·85	*1·82*	1·86	1·85	1·10
C	N	$2{\cdot}35 \times 10^{-6}$	0·081	1·96	1·97	2·00	1·99	*1·90*	1·26
	S	$5{\cdot}41 \times 10^{-7}$	0·098	1·95	2·00	2·00	*1·92*	1·94	1·20
	W	1·22	0·000	2·00	2·00	2·00	*1·98*	1·99	1·05
$\ln \alpha_s$	N	0·943	0·081	1·96	1·97	2·00	2·00	*1·81*	1·55
	S	0·467	0·208	1·90	1·94	1·89	*1·87*	1·90	1·17
	W	0·846	0·092	1·95	2·00	2·00	1·94	*1·84*	1·45
$\ln \alpha_f$	N	1·068	0·084	1·96	1·98	2·00	1·99	*1·81*	1·55
	S	0·541	0·211	1·89	1·95	1·89	*1·88*	1·89	1·17
	W	0·990	0·084	1·96	1·99	2·00	1·95	*1·84*	1·45
WI	N	1·146	0·163	1·92	1·97	2·00	1·92	*1·77*	1·70
	S	0·786	0·218	1·89	1·91	*1·89*	*1·89*	1·90	1·05
	W	1·263	0·085	1·96	1·97	2·00	1·97	*1·86*	1·38

Table II. Values of variogram parameters and fractal dimensions for TDR soil moisture data (see caption for Table I). 'Omni' denotes omnidirectional results. The lowest D value for each date is italicized

Date (1999)	Variogram (Omni)		Fractal dimension D					$10^{\Delta D}$
	a	b	Omni	10°	55°	100°	145°	
24 Jun	1·446	0·244	1·88	1·91	1·81	1·89	*1·80*	1·29
30 Jun	1·752	0·240	1·88	*1·79*	1·96	1·88	1·88	1·48
15 Jul	7·646	0·039	1·98	*1·95*	1·97	2·00	1·98	1·12
4 Aug	2·910	0·135	1·93	1·96	1·90	*1·85*	1·99	1·38
24 Sep	1·832	0·137	1·93	1·96	*1·83*	1·94	2·00	1·48

On the North field, S and WI have the largest and nearly equal magnitudes for linear regression, but they have opposite signs. The sign difference is not surprising given the definition of WI. Yet, the combination with contributing area does not improve the correlation significantly. In the case of nonlinear regression, S explains more of the variability than WI for the North field, but not for the other two fields. Across these three fields, either slope, $\ln(a_f)$ or WI provides the highest correlation with crop yield. The results are not

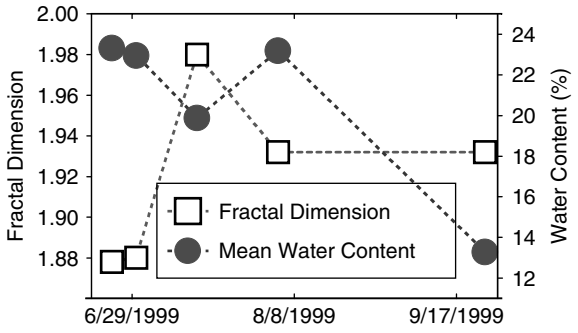

Figure 10. Time series of the fractal dimension and mean values of spatial TDR water content

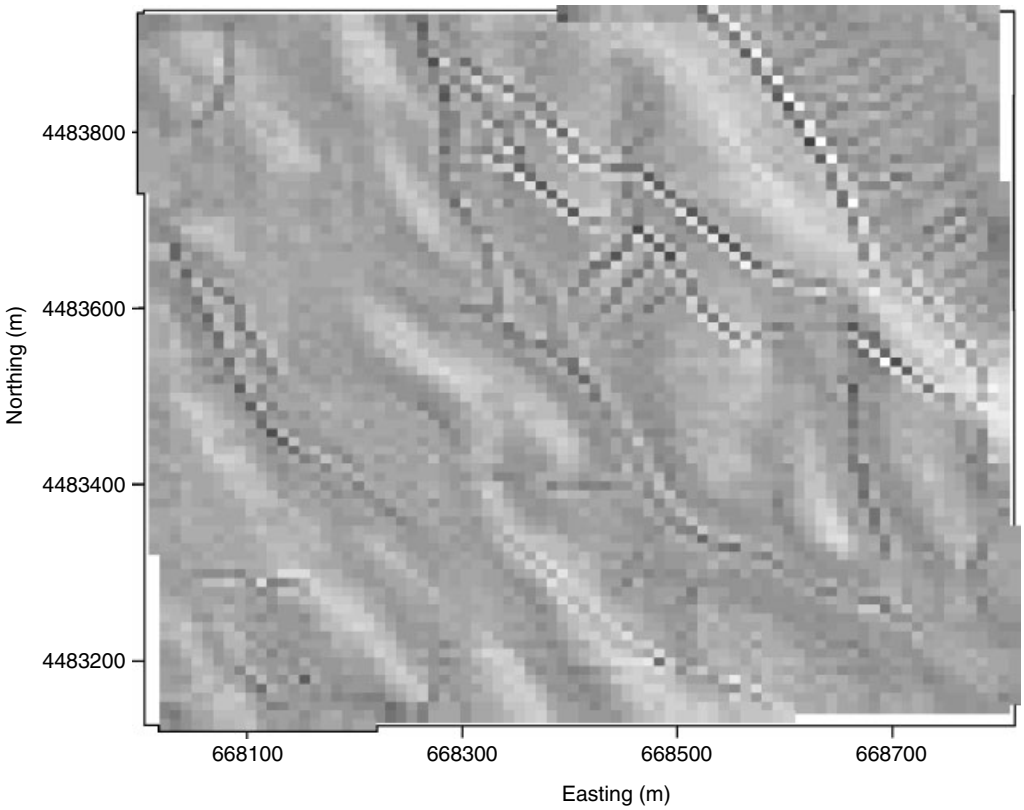

Figure 11. North field topographic curvature map. Dark is concave up (negative), and light is convex up (positive)

strictly consistent, but WI is best overall, explaining from 38 to 48% of the variability using linear regression (cf. Figure 2).

The West field is unique among these three, in that the log-transformed contributing areas have slightly greater *r*-values than WI. This coincides with the lowest magnitude of *r* for slope.

The correlations for water content (Table V) are generally much lower than for crop yield in this semi-arid landscape. For several dates, there is almost no correlation with topography. Spatial water content is most closely related to the computed topographic attributes during the wettest conditions. This is illustrated in

Table III. Ratios of variogram and fractal parameters between years (D for 1999 yield over D for 1997 yield) and between the wetness index (WI) and 1997 yield for all three fields (N = North, S = South, W = West)

Field	D(Yield99)/D(Yield97)	Ratios of WI to 1997 yield parameter values						
		a	b	D_{omni}	$D(10°)$	$D(55°)$	$D(100°)$	$D(145°)$
N	0·981[a]	3·401	0·601	1·029	1·026	1·053	1·043	0·983
S	1·000	3·107	1·112	0·994	0·990	0·984	0·990	1·027
W	0·995	2·979	0·459	1·026	0·985	1·070	1·082	0·935

[a] Foxtail millet (hay) was planted in 1999 instead of winter wheat in the North field.

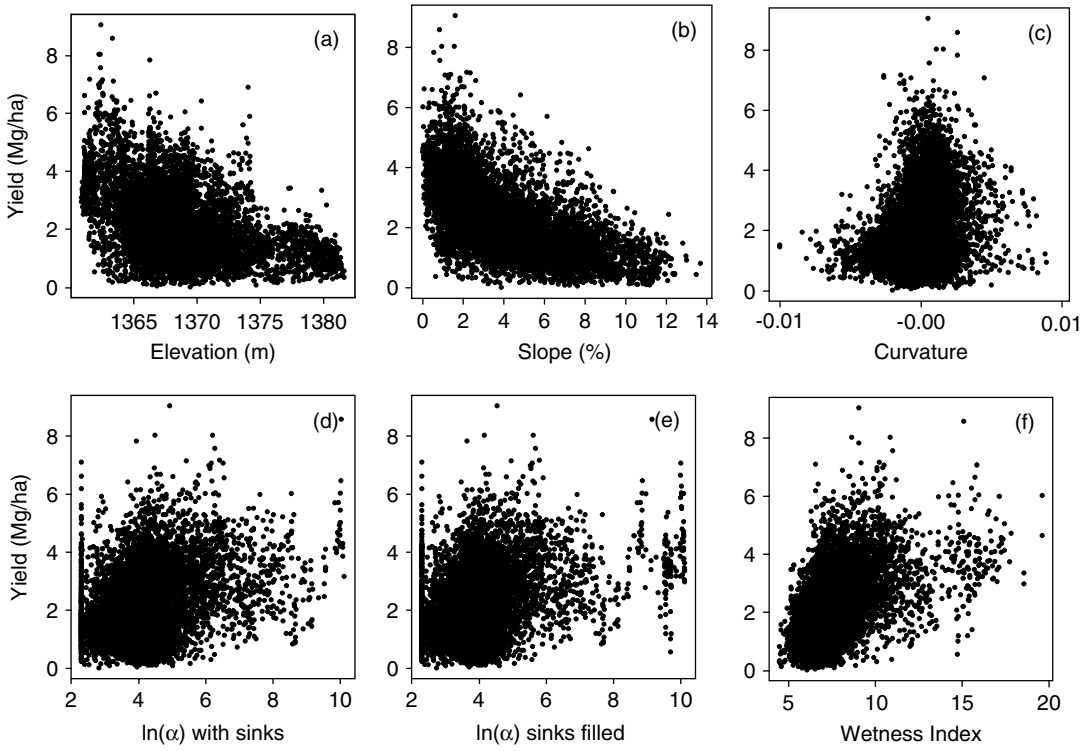

Figure 12. North field 1997 wheat grain yield versus topographic attributes from a 10 m DEM. In (d) and (e), ln(α) is the natural logarithm of the specific contributing area; in (f), wetness index is defined as ln(α/S) with sinks filled, where S is the local slope

Figure 13, where r-values of three of the strongest explanatory variables for water content (Table V) are plotted versus the mean water content for each date. The contributing area is not plotted, despite having a relatively high r-value on 27 April 2000, because it is inconsistent and even changes sign on one date. More data at the wet end are required to confirm the apparent increase in correlation compared with some of the lower moisture states shown in Figure 13. We also recall from the fractal analyses (Figure 10) that transient conditions may play a role in addition to the mean water content. Western *et al*. (1999) identified similar phenomena during transition periods from dry to wet in a more humid environment within a 10 ha pasture.

Table IV. Results of univariate regressions of crop yield on topographic attributes (North, South and West fields in 1997). See Table I for definitions of symbols for topographic attributes. Numbers in bold text are r values for linear correlation, and non-bold r values are for correlation with exponentially transformed topographic variables

Field	Crop yield (Mg ha^{-1})		Correlation coefficient r					
	Mean	SD	Z	S	C	$\ln(\alpha_s)$	$\ln(\alpha_f)$	WI
North	**2·21**	**1·26**	**−0·39**	**−0·68**	**0·36**	**0·40**	**0·40**	**0·69**
			0·53	0·76	−0·29	−0·34	−0·36	−0·66
South	**2·31**	**0·85**	**−0·13**	**−0·39**	**0·20**	**0·49**	**0·53**	**0·62**
			0·25	0·47	−0·19	−0·44	−0·48	−0·60
West	**3·11**	**1·08**	**−0·22**	**−0·10**	**0·35**	**0·65**	**0·66**	**0·63**
			0·21	0·23	−0·33	−0·64	−0·64	−0·63

Table V. Results of univariate regressions of water content on topographic attributes (North field only), where Z is elevation, S is slope, Pro C and Plan C are profile and plan curvatures, $\ln(\alpha_f)$ is specific contributing area, and WI is the wetness index, defined as $\ln(\alpha_f/S)$. Italics indicate the wettest date and highest correlations

Sample		Water content (%)		Correlation coefficient r					
Date	#	Mean	SD	Z	S	Pro C	Plan C	$\ln(\alpha_f)$	WI
30 Jun 1999	504	23·1	2·6	−0·26	−0·14	0·19	0·08	0·13	0·01
15 Jul 1999	526	19·9	3·1	−0·15	−0·09	0·00	0·04	0·00	0·13
4 Aug 1999	338	23·2	2·5	−0·06	−0·04	0·08	0·00	0·02	0·07
24 Sep 1999	589	13·3	2·1	−0·22	−0·17	0·11	0·06	0·05	0·22
27 Apr 2000	*339*	*25.9*	*1.8*	*−0.32*	*−0.45*	*0.29*	*0.17*	*0.35*	*0.24*
23 May 2000	578	20·9	2·9	−0·11	0·03	0·03	−0·03	0·00	0·02
20 Jun 2000	591	13·1	2·3	0·01	0·19	0·13	0·05	0·07	0·03
25 Jul 2000	598	14·3	2·3	−0·03	0·04	0·05	0·05	−0·06	0·04

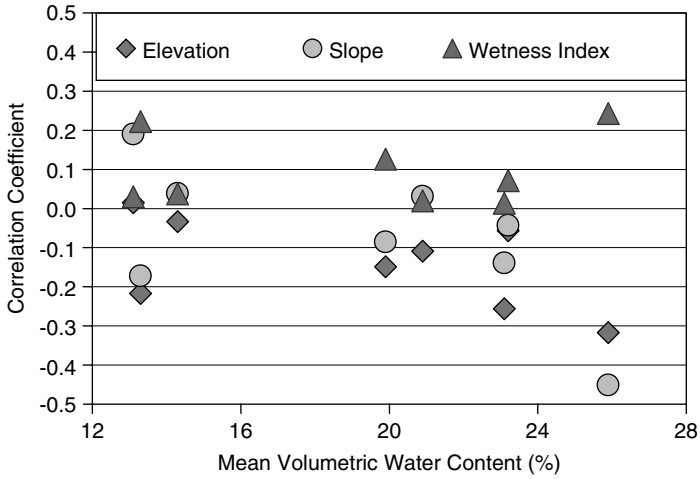

Figure 13. Values of the correlation coefficient r between TDR water content and three primary topographic attributes versus the spatial mean of water content for each sampling date (see Table V)

SUMMARY AND CONCLUSIONS

The measurement of spatial crop yield and soil-water content described here provides data needed for scaling analyses and testing of spatial correlation methods. Dryland cropping systems display large space–time variabilities that have not been explored previously using fractal analyses and detailed topographic analyses. This paper explores the data and identifies first-order relationships using univariate regression and fractal dimensions estimated from variograms. A new measure of fractal anisotropy was introduced and computed as another simple measure of spatial structure.

All of the data types (topographic attributes, crop yield, and soil-water content) display spatial structure. Experimental variograms using data in all directions out to field scales of nearly 500 m are typically nonstationary (no sill), indicating nested scales of variability consistent with fractal behaviour. This occurs despite the elevation showing a distinct sill and the variogram shape fit by the Gaussian model. In addition, some directional variograms may plateau or display periodic behaviour due to landscape undulations. The fractal dimensions computed from power-law fits to such variograms can be anisotropic. By defining the fractal dimension D based on the variance along directional transects, D ranged from 1·09 for elevation (West field at 145°) to 2·00 for certain topographic attributes and for soil-water content on two dates. Values of D for crop yield in all three fields are near 1·90, though the North field is a bit lower ($D = 1{\cdot}86$). These values fall between those of the topographic attributes, where D values for slope are somewhat lower (1·71 to 1·86) and values for the wetness index are generally higher (1·89 to 1·96). Such fractal dimensions and their anisotropy may also be useful test statistics for yield predictions from distributed crop simulation models.

The fractal dimension of topographic attributes derived from a DEM may be useful for estimating the fractal dimension of spatial crop yield in given fields within a region. Here, we found that the fractal dimension of wetness index could be used to estimate D of crop yield, and that this measure of spatial 'persistence' or smoothness was consistent from one harvest year to the next, particularly under a consistent crop rotation. Furthermore, we showed that a variogram's scale parameter a for crop yield could be estimated from that of WI for each field, where the ratio $a_{\mathrm{WI}}/a_{\mathrm{yield}} \approx 3$.

Univariate regression using topographic attributes proved useful for predicting up to half of the spatial variability in crop yield from point to point (r^2 from 0·38 to 0·48 using WI). The strongest correlations were with WI ($r = 0{\cdot}69$) and S ($r = -0{\cdot}68$ for linear regression and $r = 0{\cdot}76$ using an exponential transformation), but S was not consistent across the three fields. Yield was always negatively correlated with elevation and slope, but it was positively correlated with the others topographic attributes.

Although water content data are 'noisy', and this results in low r-values, there is spatial structure at the field scale demonstrated by the experimental variograms, particularly under relatively wet conditions. Future work will extend the present point-to-point regressions to multiple regression and nonparametric pattern matching at the field scales of interest.

ACKNOWLEDGMENTS

Michael Murphy was instrumental in all aspects of the fieldwork, and his expertise and team work are greatly appreciated. We are grateful to Gilbert Lindstrom for providing generous access to his farm for data collection. Dr Marvin Shaffer and Dr Gale Dunn initiated the on-farm cooperation and helped with yield mapping. We also appreciate the vision of Dr Lajpat Ahuja to promote the ARS work on spatial variability, his preliminary analyses of fractal behaviour on crop yield data with Dr Mahmood Nachabe, and his comments on the manuscript. We thank Daniel Salas for assistance collecting DEM and TDR data in the summers of 1999 and 2000. Finally, we thank Dr Dave Gustafson and the five anonymous journal reviewers for their careful reviews and helpful comments.

REFERENCES

Arslan S, Colvin TS. 1999. Laboratory performance of a yield monitor. *Applied Engineering in Agriculture* **15**: 189–195.

Barton CC, LaPointe RR. 1995. *Fractals in Petroleum Geology and Earth Processes*. Plenum: New York.

Beal JP, Tian LF. 2001. Time shift evaluation to improve yield map quality. *Applied Engineering in Agriculture* **17**: 385–390.

Bindlish R, Barros AP. 2002. Subpixel variability of remotely sensed soil moisture: an inter-comparison study of SAR and ESTAR. *IEEE Transactions on Geoscience and Remote Sensing* **40**: 326–337.

Blöschl G. 1999. Scaling issues in snow hydrology. *Hydrological Processes* **13**: 2149–2175.

Blöschl G, Sivapalan M. 1995. Scale issues in hydrological modeling—a review. *Hydrological Processes* **9**: 251–290.

Blöschl G, Sivapalan M, Gupta V, Beven K, Lettenmaier D. 1997. Preface to the special section on scale problems in hydrology. *Water Resources Research* **33**: 2881–2881.

Burrough PA. 1981. Fractal dimensions of landscape and other environmental data. *Nature* **294**: 240–242.

Burrough PA. 1983. Multiscale sources of spatial variation in soil, I. The application of fractal concepts to nested levels of soil variation. *Journal Soil Science* **34**: 577–597.

Cosh MH, Brutsaert W. 1999. Aspects of soil moisture variability in the Washita '92 study region. *Journal of Geophysical Research–Atmospheres* **104**: 19 751–19 757.

D'Odorico P, Rodriguez-Iturbe I. 2000. Space–time self-organization of mesoscale rainfall and soil moisture. *Advances in Water Resources* **23**: 349–357.

Erskine RH, Green TR, Dunn GH. 2001. GPS/GIS methods for collecting and analysing grain and forage data. In *Proceedings 2001 ESRI Southwestern User Group Meeting CD-ROM*, Tucson, AZ.

Gallant JC, Wilson JP. 1996. TAPES-G: a grid-based terrain analysis program for the environmental sciences. *Computers & Geosciences* **22**: 713–722.

Gerald CF. 1980. *Applied Numerical Analysis*, 2nd edn. Addison-Wesley: Menlo Park, CA.

Giloni A, Padberg M. 2002. Least trimmed squares regression, least median squares regression, and mathematical programming. *Mathematical and Computer Modelling* **35**: 1043–1060.

Hu ZL, Islam S, Cheng YZ. 1997. Statistical characterization of remotely sensed soil moisture images. *Remote Sensing of Environment* **61**: 310–318.

Hu ZL, Chen YZ, Islam S. 1998. Multiscaling properties of soil moisture images and decomposition of large- and small-scale features using wavelet transforms. *International Journal of Remote Sensing* **19**: 2451–2467.

Insightful. 2001. *S-Plus 6 for Windows Guide to Statistics*. Insightful Corp.: Seattle, WA.

Karner O. 2001. Comment on Hurst exponent. *Geophysical Research Letters* **28**: 3825–3826.

Koutsoyiannis D. 2002. The Hurst phenomenon and fractional Gaussian noise made easy. *Hydrological Sciences Journal–Journal des Sciences Hydrologiques* **47**: 573–595.

Mandelbrot B. 1977. *Fractals: Form, Chance, and Dimension*. W. H. Freeman: San Francisco.

Mayo MS, Gray JB. 1997. Elemental subsets: the building blocks of regression. *American Statistician* **51**: 122–129.

McMaster GS, Palic DB, Dunn GH. 2002. Soil management alters seedling emergence and subsequent autumn growth and yield in dryland winter wheat–fallow systems in the central Great Plains on a clay loam soil. *Soil & Tillage Research* **65**: 193–206.

Oldak A, Pachepsky Y, Jackson TJ, Rawls WJ. 2002. Statistical properties of soil moisture images revisited. *Journal of Hydrology* **255**: 12–24.

Pelletier JD, Malamud BD, Blodgett T, Turcotte DL. 1997. Scale-invariance of soil moisture variability and its implications for the frequency–size distribution of landslides. *Engineering Geology* **48**: 255–268.

Peters-Lidard CD, Pan F, Wood EF. 2001. A re-examination of modeled and measured soil moisture spatial variability and its implications for land surface modeling. *Advances in Water Resources* **24**: 1069–1083.

Peterson GA, *et al*. 2000. *Sustainable dryland agroecosystem management*. Technical Bulletin TB00-3, Agricultural Experimental Station, Colorado State University, Fort Collins, CO.

Rodriguez-Iturbe I, Vogel GK, Rigon R, Entekhabi D, Castelli F, Rinaldo A. 1995. On the spatial organization of soil moisture fields. *Geophysical Research Letters* **22**: 2757–2760.

Rodriguez-Iturbe I, D'Odorico P, Rinaldo A. 1998. Possible self-organizing dynamics for land–atmosphere interaction. *Journal of Geophysical Research–Atmospheres* **103**: 23 071–23 077.

Rousseeuw PJ. 1984. Least median of squares regression. *Journal of the American Statistical Association* **79**: 871–880.

Sposito G. 1995. Recent advances associated with soil-water in the unsaturated zone. *Reviews of Geophysics* **33**: 1059–1065.

Tarboton DG. 1997. A new method for the determination of flow directions and upslope areas in grid digital elevation models. *Water Resources Research* **33**: 309–319.

Tarboton DG. 2000. TARDEM: a suite of programs for the analysis of digital elevation data. http://www.engineering.usu.edu/dtarb/tardem.html(Accessed 23 December 2003).

Western AW, Blöschl G. 1999. On the spatial scaling of soil moisture. *Journal of Hydrology* **217**: 203–224.

Western AW, Grayson RB. 1998. The Tarrawarra data set: soil moisture patterns, soil characteristics and hydrological flux measurements. *Water Resources Research* **34**: 2765–2768.

Western AW, Grayson RB, Blöschl G, Willgoose GR, McMahon TA. 1999. Observed spatial organization of soil moisture and its relation to terrain indices. *Water Resources Research* **35**: 797–810.

Wood EF. 1995. Scaling behaviour of hydrological fluxes and variables: empirical studies using a hydrological model and remote sensing data. In *Scale Issues in Hydrological Modelling*, Kalma J, Sivapalan M (eds). John Wiley: Chichester; 89–104.

Woods RA, Sivapalan M. 1997. A connection between topographically driven runoff generation and channel network structure. *Water Resources Research* **33**: 2939–2950.